Submerged Robotic Micromanipulation and Dielectrophoretic Micro-objet release.

Michaël Gauthier, Elie Gibeau, David Hériban

Submerged Robotic Micromanipulation and Dielectrophoretic Micro-object Release

Michael Gauthier, Elie Gibeau and David Heriban
Laboratoire d'Automatique de Besançon, CNRS, ENSMM, Univ de Franche-comté
24 rue Savary, 25000 Besançon, France
E-mail: michael.gauthier@ens2m.fr, Website: www.lab.cnrs.fr

***Abstract*— The development of new hybrid microsystems needs new technologies which are able to perform assembly of small micro-objects. Now, the current micromanipulation technologies are still unreliable for micro-objects which typical size is down to hundred micrometers. Consequently, the study and the development of innovative artificial micro-object manipulation strategies in these dimensions is particularly relevant. As presented in the literature, micromanipulations are perturbed by the adhesion and surface forces which depend on surrounding mediums. We propose to perform micro-assembly tasks in liquid medium, because adhesion and surface forces applied on submerged micro-objects are less important than in air. The comparative analysis of micro-forces in air and in liquid is presented in this paper. Although the micro-forces reduce in liquid, they stay disturbed the micro-objects release. Thus, we propose to extend the dielectrophoresis micromanipulation principles which are currently done in the biological micromanipulation to submerged artificial objects micro-assembly. The negative dielectrophoresis principle is used to release a micro-object grasped with a micro-gripper. Physical principle and first experimentations is presented in this article. Further works will focus on the optimization of the principle, and on the micro-object release modelling and control.**

***Keywords*—microrobotics, micromanipulation, submerged object, dielectrophoresis.**

I. Introduction

Microrobotics research activities are different from classical robotics by the dimension of the application field: the microworld. In this scale, surface effects like electrostatic forces and pull-off force are not insignificant compared to volumic effects like weight and inertia. Below the limit of 100 micrometers, in most of cases, the surface forces are greater than the volumic forces. Consequently, the automation of micromanipulation tasks under this scale limit is particularly difficult. Surface forces are a function of the medium physical parameters like pressure, temperature, and humidity, so an automatic micromanipulation under 100 micrometers typically needs to control these physical parameters. The usual solution is to perform micromanipulations in a controlled chamber [1].

Our solution to increase the efficiency of the micromanipulations is to carry out them in a submerged medium. The choice of an electrical and thermal conductive liquid helps to easily control the medium temperature and to minimize the electrostatic perturbations. Moreover, the micromanipulation in liquid medium allows to cancel capillary forces induced by the condensation between the micro-object and the substrate [2]. Furthermore, the Hamaker constant is lower in a liquid than in air. This reduction induces a diminution of the Van-der-Waals force from 50% to 98% [3], [4], [5]. The pull-off force are also reduced in liquid. At last, like micro-objects have a small inertia, they are easily propelled to high velocity. This phenomenon usually induces the exit of micro-objects from the workspace, even the loss of these ones. In submerged medium, the hydrodynamic forces limit the micro-objects maximum velocity, so the loss of objects is avoided in liquid medium.

Moreover, every observations concerning air as a medium is also valid for vacuum. The micromanipulation in liquid medium which has many advantages compared to the dry (air or vacuum) micromanipulation is a promising research field to perform microassembly tasks.

Our works on automation of micromanipulations in liquid focus on two application fields: microassembly and the study of the interaction between biological objects and artificial objects.
First, micromanipulations of artificial objects in liquid medium can find various applications in microassembly. The complexity of microsystems is always higher and requires a lot of different materials and different microfabrication processes. Without micro-assembly technologies, it is more and more difficult to build microsystems and especially optical microsystems [6]. Consequently, the advent of new hybrid microsystems requires new micro-assembly technologies and methods. There are two main approaches in this domain: Self-assembly and robotic assembly. The first approach is useful for very large production batch but the reliability stays low [7]. The second approach is more flexible and is relevant for smaller production batch [8], [9].
Secondly, micromanipulation of artificial parts in liquid has many applications in biotechnologies. Effectively, the interaction between biological cells and artificial objects is a current biological research field. Biological studies are done to understand the interaction between bacterium and mineral particles or protein crystals [10].

In addition biocompatible studies need to observe the impact of a specific object on biological cells. Studies of the interaction between biological cell and artificial micro-objects need to position micro-objects in liquid. The automation of these studies need to guarantee a good repeatability of artificial micro-objects position in a liquid.

We present in a first part a comparison between surface forces, contact force and hydrodynamic force in air and in liquid to show the potential interest of liquid medium in micromanipulation. A specific micromanipulation strategy using dielectrophoresis is developed in a second part.

II. Theoretical Analysis

Although our approach concern liquid in general, this paper is focused on the comparison between air and water. Behavior of micro-objects is dominated by surface, contact and hydrodynamic forces rather than volume based forces. The comparative analysis of these forces in function of the medium (air or water) is developed in three parts. First, the impact of the medium on surface forces like electrostatic, van der Waals and capillary forces is presented. In case of water, hydrophobic forces, steric forces and double-layer forces has to be considered too. Secondly contact forces modelling by pull-off force in air and in water is compared. Finally the hydrodynamic effects on micromanipulations are discussed.

A. Surface Forces

1) van der Waals forces: The van der Waals forces are a well known atomic interaction force. For an interaction between a flat substrate (1) and a spherical object (2), they are equal to:

$$F_{vdw}(D) = -\frac{A_{12}R}{6D^2} \tag{1}$$

$$\text{with} \begin{cases} A_{12} \text{ Hamaker constant of the interaction (1-2)} \\ D \text{ contact distance between (1) and (2)} \\ R \text{ radius of the spherical object (2)} \end{cases}$$

The Hamaker constant A_{12} can be computed according to the constants A_{ii} of each material:

$$A_{12} \simeq \sqrt{A_{11}A_{22}} \tag{2}$$

For interaction of two materials in the presence of a third medium (3), the total force F_t to considered is expressed by the extended DLVO theory (XDLVO) proposed by Xu and Yoon [11], [12]:

$$F_t = F_{vdw} + F_{dl} + F_h \tag{3}$$

The total force is the sum of the van der Waals forces, the double-layer force and a third term which represents all other forces such as solvation, structural, hydration, hydrophobic, steric, fluctuation forces, etc. The three terms are expressed as follow:

- The van der Waals force in a third medium (3) is a function of the Hamaker constant denoted A_{132} estimated by:

$$A_{132} = A_{12} + A_{33} - A_{13} - A_{23} \tag{4}$$
$$\simeq (\sqrt{A_{11}} - \sqrt{A_{33}})(\sqrt{A_{22}} - \sqrt{A_{33}}) \tag{5}$$

- The repulsive double layer force F_{dl} can be currently written as [13], [14], [15]:

$$F_{dl} \simeq 4\pi R\epsilon_3\kappa_3\Phi_1\Phi_2 e^{-\kappa_3 D} \tag{6}$$

  where ϵ_3 is the dielectric constant of the medium, Φ_1, Φ_2 are the surface potentials of the sphere and the surface and κ_3 the Debye length of the medium. The repulsive double layer force F_{dl} is typically greater than the van der Waals force between $D = 1\,nm$ to $D = 10 - 20\,nm$ [13]. This repulsive force is able to reduce in this range the impact of the van der Waals force.
- The third term represents notably the solvation forces which have typically significant impact at very small range lower than $10\,nm$. In water, these force is repulsive for hydrophilic surface and attractive for hydrophobic surface [13]. In case of hydrophilic surface this force is able to reduce the impact of the van der Waals force.

Table I gives the values of Hamaker constant for some materials in vacuum and in water. The immersion is then able to reduce the van der Waals forces. However, these forces have a short range (typically $< 100\,nm$) compared to the size of the object (greater than $1\,\mu m$). The impact of these forces on the micro-objects behaviour is thus limited compared to very long range of electrostatic interactions and compared to contact forces.

Materials	Vacuum	Water
Gold	40	30
Silver	50	40
Al_2O_3	16.8	4.4
Copper	40	30

TABLE I

Values of Hamaker constant for some materials $A \times 10^{-20} J$ [16]

2) Electrostatic Forces: The force applied by an electrostatic surface (σ_1 surface charge density) on an electric charged particle (q_2) is given by:

$$F_e = \frac{q_2\sigma_1}{2\epsilon_3} \tag{7}$$

Comparison of dielectric constants between water and air is presented in table II. The water dielectric constant is more important than the air dielectric constant. So, in the same electrical charges configuration (q_2, σ_1) electrostatic force is significantly reduced in water.

Moreover electrostatic perturbations observed in micromanipulation are caused by tribo-electrification. During a microassembly task, friction between manipulated objects induces electric charges on the objects surface. The charge density depends on the tribo-electrification and conductivity of the medium. Effectively, a higher electric conductivity medium is able to discharge objects' surfaces. Water, especially ionic water, has better electric conductivity than air (table II). Consequently, charge density in water is reduced. The electrostatic force directly proportional to the charge density σ_1 is therefore reduced.

Electric parameters	**Air**	**Water**
Dielectric constant ε	~ 1	80.4
Conductivity	$10^{-7}\,S.m^{-1}$	$> 10^{-4}\,S.m^{-1}$

TABLE II

Relative dielectric constant and electrical conductivity of air and water

Both impact of the immersion on electric properties of the medium (dielectric constant and conductivity) induces a reduction of electrostatic forces. In conclusion, electrostatic perturbations are highly reduced in water compared to the air.

3) Capillary Forces: The capillary phenomenon between an object and a substrate in air can be described by a liquid bridge presented in figure 1 characterized by a volume V, a liquid surface tension γ and wettability properties defined by the contact angles θ_1 and θ_2. With the assumptions that the equality of the contact angles $\theta_1 = \theta_2 = \theta$, a constant volume and a small immersion height (D), capillary force between a plan and sphere (radius R) is equal to [13]:

$$F_c = \frac{4\pi R\gamma\cos\theta}{1 + (D/d)} \tag{8}$$

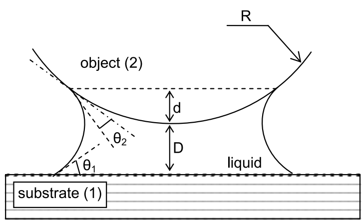

Fig. 1. Liquid meniscus formation between a spherical object and a substrate.

This capillary force is induced by the surface between the liquid and the air near to the object. In a liquid this surface disappears, so this force is cancelled in a liquid medium.

B. Contact Forces

The pull-off force represents the required force to break the contact surface between two objects. In case of a sphere (radius R) on a planar surface, pull-off force F_{PO} is approximately given by JKR [17] (for the lower boundary) or DMT [18] (for the higher boundary) contact models:

$$\frac{3}{2}\pi R W_{12} \leq F_{PO} \leq 2\pi R W_{12} \tag{9}$$

where W_{12} is the work of adhesion between both objects (1) and (2). In air, the work of adhesion is expressed by:

$$W_{12} = \gamma_1 + \gamma_2 - \gamma_{12} \simeq 2\sqrt{\gamma_1\gamma_2} \tag{10}$$

with $\begin{cases} \gamma_{12}\text{: interfacial energy} \\ \gamma_1,\ \gamma_2\text{: surface energy of the object, substrate or tip} \end{cases}$

In case of the objects are submerged in medium (3), the surface energy, denoted W_{132}, required to separate two objects (1) and (2) submerged in a medium (3) is given by:

$$W_{132} = W_{12} + W_{33} - W_{13} - W_{23} \simeq \gamma_{13} + \gamma_{23} - \gamma_{12} \tag{11}$$

For example, in case of a SiO_2-SiO_2 contact ($\gamma_{SiO_2} = 290\ mJ.m^{-1}$ [16]), the theoretical surface energies in air and in water are (from (10), (11)):

$$W_{12} = 580\,mJ.m^{-1} \quad W_{132} = 146\,mJ.m^{-1} \tag{12}$$

In this example, the pull-off force is reduced in water compared to the air. Usually, solid state surface energy are around $1000\,mJ.m^{-1}$ and the theoretical pull-off reduction is around 50% to 80%.

C. Impact of the Hydrodynamic Forces on the Micro-objects Behaviour

In this section the impact of the hydrodynamic forces on the micro-objects behaviour is described. In the micro-world, the Reynolds number which characterizes the liquid flow is usually very low (< 1). The flow is thus highly laminar. In case of a micro-object placed in an uniform liquid flow, the Stokes law directly gives the hydrodynamic force applied on the object. This law is valid when the flow Reynolds number is lower than 1 and can be extrapolated to Reynolds number lower than 10 with a good approximation.

The Stokes law defines the force applied on an object in a uniform flow of fluid defined by a dynamic viscosity μ and a velocity V:

$$\overrightarrow{F}_{drag} = -k.\mu.\overrightarrow{V} \tag{13}$$

with k a function of the geometry

eg: $k = 6\pi R$ in case of a sphere - radius R

Table III gives the values of dynamic viscosity μ of both water and air. Then the hydrodynamic force proportional to the dynamic viscosity highly increases in a submerged medium.

As inertial effects are very small in the micro-world, micro-objects acceleration is usually very high. In this way, micro-objects velocity is able to increase in a very short time. Consequently, a micro-object can reach an

Dynamic viscosity	Water	Air
μ $[kg.m^{-1}.s^{-1}]$	10^{-3}	$18.5\,10^{-6}$

TABLE III

Dynamic viscosity of water and air, $T^{o} = 20^{o}C$

high velocity, and object trajectory could be difficult to control especially in case of a visual feedback. In fact, the object can jump rapidly out of the field of view which could induce its loss. So, in most cases, velocity limitation in the submerged micro-world does not depend on inertial physical limitation but on hydrodynamic physical limitation. From this, a liquid medium is able to reduce maximal micro-objects velocity [19]. Consequently, the increasing of hydrodynamic force is able to limit the maximal velocity of the objects and thus significantly reduces the micro-objects losses.

However, movements of liquid induced by the movement of the effector are able to lead to significant hydrodynamic force on micro-objects. Consequently to avoid disturbance on micro-objects the maximum velocity of the effector has to be limited. Nevertheless, experimentally the maximum velocity of the effector can stay high (eg. $1\,mm.s^{-1}$) compared to the typical size of the object manipulated ($50\,\mu m$).

D. Synthesis

In conclusion, contact, non contact and hydrodynamic force were presented in both liquid and dry media. This analysis shows the reduction of contact and non contact forces in a liquid compared to the air. As these effects are able to perturb the micromanipulation tasks, the use of a liquid could improve the efficiency of micromanipulation. Moreover, the increase of the hydrodynamic effects is beneficial to the micro-objects behaviour during their micromanipulation. Thus, the theoretical study shows the interest of submerged media for such tasks. Comparisons of force measurement in air and in water, and experimental microgripping tests were performed and are presented in [20].

III. Dielectrophoretic Release

Though the adhesion forces are reduced in liquid, sticking effects are not totally cancelled[20] and the release task stays a critical problem. Thus the study of new release strategies of artificial micro-objects in liquid is a key-point to perform submerged micro-assembly. In the current micromanipulations, usual approaches consist in control of a repulsive physical force to overcome the pull-off force (eg. acceleration in air [21]).

We propose to use repulsive dielectrophoretic force to overcome pull-off force to control the release of the micro-objects. This principle usually used in biological cell manipulations is easily controllable by an electric field and is particularly efficient in liquid.

A. Principle of Dielectrophoresis

The time averaged dielectrophoretic force F_{DEP} and torque T_{DEP} applied by a particle in an inhomogeneous electric field $\overrightarrow{E}(t)$ is expressed by [22]:

$$\vec{F}_{DEP} = K_g.K_{DEP}.\epsilon_3.\vec{\nabla}E(rms)^2 \quad (14)$$

$$\vec{T}_{DEP} = K_g.K'_{DEP}.\epsilon_3.(E_x^2 \bigtriangledown \phi_x + E_y^2 \bigtriangledown \phi_y + E_z^2 \bigtriangledown \phi_z) \quad (15)$$

where $E(rms)$ is the rms value of the electric field strength, E_i and ϕ_i are the magnitude and phase of the field components in the axis i and K_g is a function of the geometry of the particle. For example in case of a spherical micro-object with a diameter r_2, K_g is expressed by:

$$K_g = 2\pi r_2^3 \quad (16)$$

The parameters K_{DEP} and K'_{DEP} is the real part and the imaginary part of the complex Clausius-Mosotti parameter. These parameters characterise the electric behaviour of the particle and the medium and are expressed by:

$$K_{DEP} = Re\left(\frac{\kappa_2 - \kappa_3}{\kappa_2 + 2.\kappa_3}\right) \quad (17)$$

$$K'_{DEP} = Im\left(\frac{\kappa_2 - \kappa_3}{\kappa_2 + 2.\kappa_3}\right) \quad (18)$$

where
$$\begin{cases} \kappa_2 & = \epsilon_2 - j\sigma_2/\omega \\ \kappa_3 & = \epsilon_3 - j\sigma_3/\omega \\ \epsilon_2 & : \text{dielectric constant of the particle} \\ \epsilon_3 & : \text{dielectric constant of the medium} \\ \sigma_2 & : \text{conductivity of the particle} \\ \sigma_3 & : \text{conductivity of the medium} \\ \omega & : \text{angular frequency of the electric field} \end{cases}$$

If the K_{DEP} parameter is positif, microparticle tends to move to the highest electric field gradient (near to the electrode). The dielectrophoretic force is attractive and is called 'positive-DEP'. In case of a negative K_{DEP}, microparticle tends to move to the lowest electric field (far from the electrode). The dielectrophoresis force is repulsive and is called 'negative-DEP'.

The dielectrophresis (DEP) is usually used in cell micromanipulation to perform direct cell sorting [23][24] or field-flow-fractionation (FFF-DEP) [25][26]. In specific configurations, it allows to catch individual cells too [27]. Moreover dielectrophoresis is used to manipulate Carbon Nano Tubes (CNT) in the field of nanomanipulation [28]. Although this principle is not really effective in air, recently Subramanian presents first tests on the use of DEP in artificial objects manipulation in air [28]. In this medium, this kind of physical principle requires high voltage (eg. 200V).

Considering the submerged micro-objects manipulation is relevant and the DEP is particularly effective in liquid, we propose to apply this principle to submerged artificial micro-objects manipulation.

B. Robotic Micro-manipulation using Dielectrophoresis

1) Principle: The principle proposed is an original way to perform artificial micro-objects positioning. As the grasping by a gripper with two fingers allows to induce complex 3D trajectories and complex microassembly task (ie. insertion), we choose to manipulate micro-objects with a two fingers gripper. Consequently the release task is perturbed by the adhesion force (pull-off force). We propose to use negative dielectrophoresis to control the micro-object release. Electric field could be produced by electrodes placed on the gripper or by using a conductive micro-gripper. After opening the gripper, an alternative electric field is applied on the gripper electrodes and induces a repulsive force on the micro-object whose objective is to release the object.

The behaviour of the micro-object is composed of two phases:

- The micro-object is in contact with the gripper and is immobile (Fig 2(a)) .
- The micro-object is in motion in the liquid (Fig 2(b)) .

Before the release, forces applied to the micro-object is the adhesion force and the dielectrophoresis force. The release appears if the dielectrophoresis is greater than the pull-off force:

$$F_{DEP} > F_{PO} \qquad (19)$$

After the release, in a very short time the micro-object reaches its maximum velocity. The micro-object trajectory is then defined by the equilibrium of the dielectrophoretic force and the hydrodynamic force F_{drag} induced by the liquid.

$$\overrightarrow{F}_{DEP} = -\overrightarrow{F}_{drag} \qquad (20)$$

Consequently from (13) the trajectory of the particle is defined by its velocity $\overrightarrow{V}$:

$$\overrightarrow{V} = \frac{1}{k.\mu}\overrightarrow{F}_{DEP} \qquad (21)$$

The transition (acceleration of the micro-object) between both cases is made in a very short time (ie. $50\mu s$) because of the small inertia of the micro-object. As the precise description of this acceleration phase has no specific interest in micromanipulation, the complete behaviour of the micro-object is described by the equations (19-21).

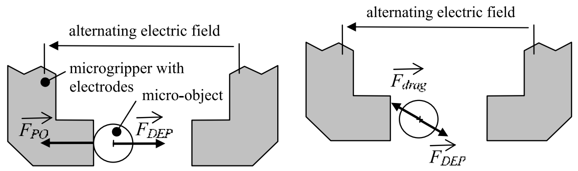

(a) First step: the dielectrophoretic force F_{DEP} overcome the pull-off force F_{PO}

(b) Second step: the dielectrophoretic force F_{DEP} is opposed to drag force F_{drag}

Fig. 2. Principle of the dielectrophoretic release

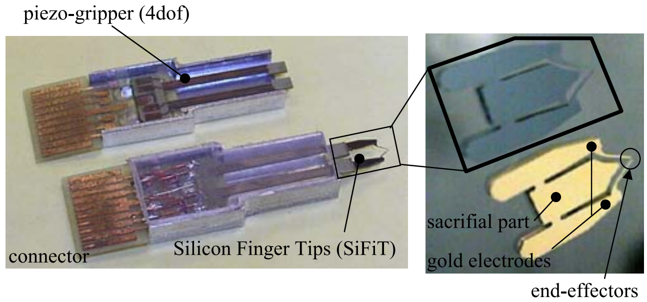

Fig. 3. Piezo-microgripper and Silicon Finger Tips (SiFiT)

2) Experimentations: To valid our approach, experimentations were performed on glass microsphere with a diameter $20\,\mu m$. The gripper is a four Degree Of Freedom (DOF) piezoelectric microgripper described in [29]. Specific end-effectors in Silicon were build with microfabrication technologies (D-RIE) and glued on the microgripper as presented in [29]. The silicon end-effectors and micro-gripper is presented in Figure 3. Thickness of the end-effectors is $12\,\mu m$ and the shape is presented in Figure 4. Gold electrodes are sputtered on the silicon end-effectors to applied alternating electric field.

An example of glass micro-sphere release is presented in Figure 4. The electric voltage used was a sinusoidal signal $\pm 20V$ peak-to-peak. The release and the trajectory of the micro-object is visible in Figure 4.

Experimentations show a high reliability on glass micro-object releases. The control of the release is easy to perform via the tension of electrodes. This first result demonstrates the interest in using dielectrophoresis release in submerged micromanipulations.

However at present, the final position of the released micro-object is not controlled. Further works will be done to purchase the modeling of the micro-object behaviour after the release to control its final position. The shape, number, and architecture of electrodes will be studied and tested to optimize and control this release principle.

IV. Conclusion

As the development of new hybrid microsystems requires new micro-assembly technologies, the study of in-

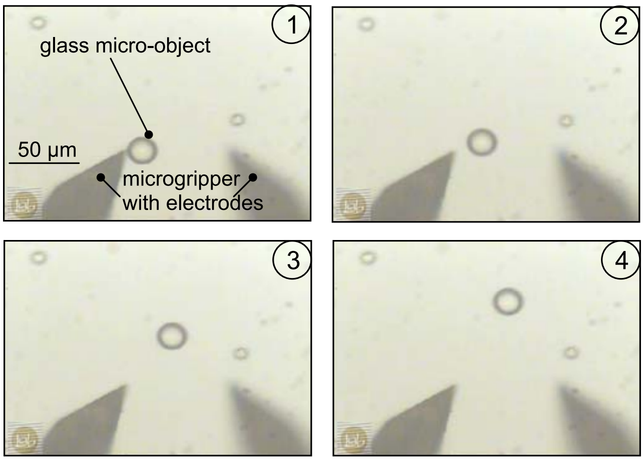

Fig. 4. Experimental DEP release

novative ways to perform micro-objects assembly is particularly relevant. The reduction of the impact of adhesion and surface forces on the manipulated objects behaviour is a keypoint to increase the reliability of current micromanipulation strategies. The theoretical analysis presented in this paper shows that adhesion and surface forces are reduced in water compared to the air. Consequently, micromanipulation in liquid medium is a potential way to ease micro-objects assembly. Impact of the adhesion and surface forces on micro-objects behaviours are reduced but not really cancelled and the release task stays a critical point in liquid. We propose to use negative (repulsive) dielectrophoretic force to control the release of the object. The description of this new artificial objects micromanipulation principle was described in this paper and experimentations show the reliability of this strategy. Further works will focus on the optimization of the principle, and on the micro-object release modelling and control.

References

[1] Q. Zhou, B. Chang, and H. N. Koivo. Ambient environment effects in micro/nano handling. In *Proc. of the Int. Workshop on Microfactories*, pages 146–51, Shangai, China, October 2004.

[2] X. Xiong, S.-H Liang, and K. F. Böhringer. Geometric binding site design for surface-tension driven self-assembly. In *Proceedings of the 2004 IEEE ICRA*, pages 1141–48, New Orleans, USA, April 2004.

[3] H. D. Ackler, R. H. French, and Y. M. Chiang. Comparison of hamaker constants for ceramic systems with intervening vacuum or water from force laws and physical properties. *Journal of Colloid and Interface Science*, 179:460–69, 1996.

[4] R. H. French. Origins and applications of london dispersion forces and hamaker constants in ceramics. *Centennial Feature Article, Journal of the American Ceramic Society*, 83(9):2117–49, 2000.

[5] A. L. Weinsenhorn, P. K. Hansma, T. R. Albrecht, and C. F. Quate. Forces in atomic force microscopy in air and water. *Appl. Phys. Lett.*, 54:2651–53, 1989.

[6] H. Van Brussel, J. Peirs, D. Reynaerts, A. Delchambre, G. Reinhart, N. Roth, M. Weck, and E. Zussman. Assembly of microsystems. *Annals of the CIRP*, 49(2):451–472, 2000.

[7] George M. Whitesides and Mila Boncheva. Beyond molecules: Self-assembly of mesoscopic and macroscopic components. *Proceedings of the National Academy of Sciences of the United States of America*, 99(8):4769–4774, 2002.

[8] T. Udeshi and K. Tsui. Assembly sequence planning for automated micro assembly. In *International Symposium on Assembly and Task Planning*, 2005.

[9] N. Dechev, W. L. Cleghorn, and J. K. Mills. Microassembly of 3d microstructures using a compliant, passive microgripper. *Journal of Microelectromechanical Systems*, 13(2), April 2004.

[10] Atanas Georgiev, Peter K. Allen, and William Edstrom. Visually-guided protein crystal manipulation using micromachined silicon tools. In *Proceedings of 2004 IEEE/RSJ International Conference on Intelligent Robots and Systems*, pages 236–41, Sendai, Japan, Oct. 2004.

[11] Z. Xu and R. H. Yoon. The role of hydrophobic interactions in coagulation,. *J. Colloid Interface Sci.*, 44(132):532–541, 1989.

[12] Z. Xu and R.H. Yoon. A study of hydrophobic coagulation. *J. Colloid Interface Sci.*, 45(134):427–434, 1990.

[13] J. Israelachvili. *Intermolecular and Surface Forces*. Academic Press, 1991.

[14] X-Y Lin, F. Creuset, and H. Arribart. Atomic force microscopy for local characterzation of surface acid-base properties. *J. Phys. Chem.*, 97:7272–76, 1993.

[15] Nehal I. Abu-Lail and Terri A. Camesano. Role of ionic strength on the relationship of biopolymer conformation, dlvo contributions, and steric interactions to bioadhesion of pseudomonas putida kt2442. *Biomacromolecules*, 4:1000–12, 2003.

[16] D. S. Rimai and D. J. Quesnel. *Fundamentals of Particle Adhesion*. Adhesion Society, 2001.

[17] J.A. Greenwood K.L. Johnson. An adhesion map for the contact of elastic spheres. *J. Colloid Interface Sci.*, 192(2):326–333, 1997.

[18] B. V. Derjaguin, V.M. Muller, and YU. P. Toporov. effect of contact deformations on the adhesion of particles. *Journal of Colloid and interface science*, 53(2):314–326, 1975.

[19] M. Gauthier, B. Lopez-Walle, and C. Clévy. Comparison between micro-objects manipulations in dry and liquid mediums. In *proc. of CIRA'05*, June 2005.

[20] M. Gauthier, S. Régnier, P. Rougeot, and N. Chaillet. Forces analysis for micromanipulations in dry and liquid media. *Journal of Micromechatronics*, 3(3-4):389–413, Sept. 2006.

[21] D. S. Haliyo and S. Régnier. Advanced applications using ţmad, the adhesion based dynamic micro-manipulator. In *Proceedings of the 2003 IEEE/ASME Int. Conf. on Advanced Intelligent Mechatronics (AIM 2003)*, pages 880–85, Port Island, Kobe, Japan, July 2003.

[22] P. Gascoyne, X. Wang, Y. Huang, and F. Becker. Dielectrophoretic separation of cancer cells from blood. In *IEEE Proc.*, pages 1366–1373, 1995.

[23] Frederick F. Becker, Peter R.C. Gascoyne, Ying Huang, and Xiao-Bo Wang. *Method and appartus for manipulation using spiral electrodes*. United States Patent, Patent Number US 5 858 192, 12 janv 1999.

[24] N. Tsukada, K. Kudoh, A. Yamamoto, T. Higuchi, M. Kobayashi, K. Sato, K. Oishi, and K. Iida. Development of oocyte rotation system for biological cell manipulation. In *Proc of the 32nd International Symposium on Robotics - ISR2001*, Seoul - Korea, 19-21 April 2001.

[25] P. Gascoyne and J. Vikoukal. Dielectrophoresis-based sample handling in general-purpose programmable diagnostic instruments. *IEEE Proceedings*, (1):22 – 42, 2004.

[26] M. Frenea, S. P. Faure, B. Le Pioufle, Ph. Coquet, and H. Fujita. Positioning living cells on a high-density electrode array by negative dielectrophoresis. *Materials Science and Engineering*, 23:597–603, 2003.

[27] A. Rosenthal and J. Voldman. Dielectrophoretic traps for single-particle patterning. *Biophysical Journal*, 88, march 2005.

[28] A Subramanian, B Vikramaditya, B J Nelson, D J Bell, and L Dong. Dielectrophoretic micro/nanoassembly with microtweezers and nanoelectrodes. In *Proc. of the 12th Int. Conf. on Advanced Robotics, Seattle*, July 2005.

[29] David Heriban, Joël Agnus, Jean-René Coudevylle, Michaël Gauthier, and Nicolas Chaillet. Design of silicon finger tips for

a moc (microrobot on chip) microgripper. In *Proc. of the Int. Workshop on Topica Meeting on Microfactories (TMMF05)*, Tsukuba, Japan, October 2005.